NANO LETTERS

2008
Vol. 8, No. 6
1762-1770

Exponential Growth of LBL Films with Incorporated Inorganic Sheets

Paul Podsiadlo,[†] Marc Michel,[†] Jungwoo Lee,[‡] Eric Verploegen,[+] Nadine Wong Shi Kam,[†] Vincent Ball,[⊗] Jaebeom Lee,[#] Ying Qi,[§,⊥] A. John Hart,[||] Paula T. Hammond,[¶] and Nicholas A. Kotov*[,†,‡,§]

Departments of Chemical Engineering, Biomedical Engineering, Materials Science and Engineering, Mechanical Engineering, and Electron Microbeam Analysis Laboratory, University of Michigan, Ann Arbor, Michigan 48109, Department of Nanomedical Engineering, Pusan National University, Busan, South Korea, Department of Chemical Engineering and Department of Materials Science and Engineering, Massachusetts Institute of Technology, Cambridge, Massachusetts 02139, and Institut National de la Santé et de la Recherche Médicale, Unité Mixte de Recherche 595, Université Louis Pasteur-Faculté de Chirurgie Dentaire, 11 rue Humann, 67085 Strasbourg Cédex, France

Received April 24, 2008

ABSTRACT

The fastest growth pattern of layer-by-layer (LBL) assembled films is exponential LBL (e-LBL), which has both fundamental and practical importance. It is associated with "in-and-out" diffusion of flexible polymers and thus was considered to be impossible for films containing clay sheets with strong barrier function, preventing diffusion. Here, we demonstrate that e-LBL for inorganic sheets is possible in a complex tricomponent film of poly(ethyleneimine) (PEI), poly(acrylic acid) (PAA), and Na^+-montmorillonite (MTM). This system displayed clear e-LBL patterns in terms of both initial accumulation of materials and unusually thick individual bilayers later in the deposition process with film thicknesses reaching 200 μm for films composed of 200 pairs of layers. Successful incorporation of MTM layers was observed by scanning electron microscopy and thermo-gravimetric analysis. Surprisingly, the growth rate was found to be nearly identical in films with and without clay layers, which suggests fast permeation/reptation of polyelectrolytes between the nanosheets during the "in-and-out" diffusion of polymer. In considering these findings, e-LBL growth property is expected for a wide array of available inorganic nanoscale components and have a potential to greatly expand the e-LBL field and LBL field altogether. The large thickness and rapid growth of the films affords fast preparation of nanostructured materials which is essential for multiple practical applications ranging from optical devices to ultrastrong composites.

Preparation of multilayered nanostructured thin films with the layer-by-layer (LBL) assembly technique has gained wide popularity in the past decade. Since the first demonstration of LBL assembly for oppositely charged microparticles by Iler[1] and later by Decher et al. in the 1990s for oppositely charged polyelectrolytes,[2,3] the LBL field has experienced rapid growth. The technique has quickly become one of the most popular and well-established methods for the preparation of multifunctional thin films thanks to its simplicity, robustness, and versatility.[4] Subsequent introduction of hybrid films, for example, organic/inorganic among the others, has further enriched the functionality and applicability of LBL. It has been shown that nearly any type of macromolecular species, including inorganic molecular clusters,[5] nanoparticles,[6] nanotubes and nanowires,[7,8] nanoplates,[9] organic dyes,[10] organic nanocrystals,[11,12] dendrimers,[13] porphyrin,[14] polysaccharides,[15,16] polypeptides,[17] nucleic acids and DNA,[18] proteins,[19,20] and viruses,[21] can be successfully used as assembly components.[22] In our opinion, the high molecular weight of the species being assembled is the most unifying property of this technique.[23] Remarkable versatility has further led to a number of novel designs and applications, for example, superhydrophobic surfaces,[24,25] chemical sensors and semipermeable membranes,[22,26–28] drug and biomolecules delivery systems,[22,29,30] memory devices,[31] optically active and responsive films,[12,32–34] cell and protein adhesion resistant coatings,[22,35] fuel cells and photovoltaic materials,[36] biomimetic and bioresponsive coatings,[25,37] semiconductors,[38,39] catalysts,[40,41] magnetic devices,[42,43] and many more.[4,22]

Given their wide applicability, preparation of the films has also stimulated a large number of studies aimed at the understanding of their physicochemical formation mechanisms.

* To whom correspondence should be addressed. Phonr: (734) 763-8768. Fax: (734) 764-7453. E-mail: kotov@umich.edu.
[†] Departments of Chemical Engineering, University of Michigan.
[‡] Biomedical Engineering, University of Michigan.
[§] Materials Science and Engineering, University of Michigan.
[||] Mechanical Engineering, University of Michigan.
[⊥] Electron Microbeam Analysis Laboratory, University of Michigan.
[#] Pusan National University.
[¶] Department of Chemical Engineering, Massachusetts Institute of Technology.
[+] Department of Materials Science and Engineering, Massachusetts Institute of Technology.
[⊗] Université Louis Pasteur-Faculté de Chirurgie Dentaire.

10.1021/nl8011648 CCC: $40.75
Published on Web 05/17/2008

While a vast majority of LBL systems undergo linear growth (l-LBL), there are also some quite special combinations of polyelectrolytes which exhibit so-called "exponential growth" (e-LBL). Recently, a different modification of the technique which does not require rinsing and is based on dewetting phenomena, so-called dewetting LBL or d-LBL, was also introduced by our group.[44] The l-LBL method has been studied and applied most extensively and thus covers most of LBL publications. A substantially smaller and more recent subset of LBL literature is related to e-LBL films. Historically, e-LBL was observed for the first time in 1999 by Elbert et al.[45] for poly(L-lysine) (PLL) and alginate (AG) polyelectrolytes pair. The authors observed that the thickness of dried films increased exponentially with the number of deposited layers. To explain the results the authors have evoked a possibility of formation of a PLL/AG complex coacervate, a type of gel, on the film surface during the successive deposition. Subsequently, Ruths et al.[46] observed exponential growth in a polystyrene sulfonate (PSS)/polyallylamine (PAH) multilayer assembled onto a Langmuir monolayer which they have attributed to increasing film roughness with increasing thickness. Pardo-Yissar et al.[47] have also observed nonlinear buildup of a PLL/poly(acrylic acid) (PAA) multilayer system, and their explanation was the swelling of the film and increased absorbance of water. Finally, Picart et al.[48,49] and Lavalle et al.[50–52] have suggested a formation mechanism and later presented a proof of an "in-and-out" diffusion of the polyelectrolytes. In the studied system, the authors have found that the polycation diffuses into the film during the deposition, then out of the film during rinsing, and further out during polyanion deposition. When immersed into the polyanion solution, as the diffusing polycation reaches the outer surface of the film, it interacts with the incoming polyanion to form a polycation/polyanion complex layer. The thickness of this new layer was found to be proportional to the amount of the polycation that diffused out of the film.

The fundamental understanding of the growth mechanism has spurred development of novel structures and applications of the resulting films. For example, Boulmedais et al.[17] have shown controlled switching of random-to-α-helical structure of poly(L-glutamic acid) (PLGA) in a PLGA/PAH e-LBL. Garza et al.[53,54] have also shown preparation of multicompartment e-LBL films while Hübsch et al.[55] and later others[56] have shown the ability to control the l-LBL versus e-LBL growth behavior of the films. The e-LBL films have also shown interesting stability dependence in response to ferrocyanide and ferricyanide ions.[57,58] Kujawa et al. and others have shown dependence of the e-LBL film thickness on the molecular weight of the polyelectrolytes.[59,60] The e-LBL interdiffusion of polyelectrolytes have been shown to induce spontaneous ordering and exchange of viruses incorporated in the films,[21] which has been applied to the formation of battery electrodes by Nam et al.[61] Most recently, several novel applications of e-LBL have been presented. These include strengthening of wood fibers,[62] drug and DNA delivery platforms,[63–66] preparation of superhydrophobic surfaces,[67] mechanically responsive nanovalves,[68] and a novel platform for spontaneous assembly of rod-shaped viruses.[21]

One can quickly notice that all of the above-mentioned e-LBL structures were based on purely polymeric or organic precursors. The types of polyelectrolyte pairs engaged in e-LBL thus appear to be limited, while it would be quite interesting to expand the functionality of the exponentially grown films to a greater number of LBL-capable species mentioned above. As such, it would be very interesting to include nanoscale inorganic components in the e-LBL films, for instance, nanosheets of Na^+-motmorillonite (MTM). These sheets produce composites with unusually high mechanical properties similar to those of seashell nacre and lamellar bones.[69] In fact, the mechanical properties of this material (ultimate tensile strength, $\sigma_{UTS} = 100 \pm 10$ MPa and the Young's modulus, $E = 11 \pm 2$ GPa) exceed those of many clay composites prepared by simple dispersion and that gave a precedence for studying these structures for preparation of ultrastrong composites.[70,71] As a result, in a recent report, we have shown preparation of a transparent clay nanocomposite with record-high strength and stiffness for this class of materials: $\sigma_{UTS} = 400 \pm 40$ MPa and $E = 106 \pm 11$ GPa.[72] The ability of MTM to work as nanoscale armor for other types of nanoparticles was also used in assemblies of MTM and magnetite or Ag NPs films.[43,73] LBL films utilizing insulating functionality of alumosilicate sheets were made with gold NPs.[74] Other examples of LBL assemblies incorporating MTM nanosheets include preparation of LBL films of myoglobin or horseradish peroxide for voltammetry studies, photocontrollable magnetic thin films, chemiluminescent thin films for sensory applications, or perm-selective membranes.[75–80]

In many of these cases, and for nacre-like composites especially, it would be useful if MTM multilayers formed faster as in exponential growth mode. We have asked a question of whether it is actually feasible to generate hybrid organic/inorganic e-LBL films. The conundrum here is that MTM films have been shown to produce very effective diffusion barriers,[81] which are expected to strongly hinder the diffusion in the LBL films. According to the current understanding of the e-LBL mechanism, this should make e-LBL impossible. To our great surprise, this understanding is not true and MTM does allow for the "in-and-out" diffusion process of macromolecules to occur.

Here, we present results from e-LBL assembly of a hybrid system composed of poly(ethyleneimine) (PEI), poly(acrylic acid) (PAA), and MTM with the following deposition sequence: $(PEI/PAA/PEI/MTM)_n$, where n is the number of deposition cycles, and in this tricomponent system, it corresponds to 2 pairs (bilayers) of oppositely charged compounds per cycle. The assembly and film architecture was characterized with scanning electron microscopy (SEM), small-angle X-ray scattering (SAXS), and laser scanning confocal microscopy, and it was compared with its organic counterpart, that is, $(PEI/PAA)_n$ and a "nacre-like" analogue $(PEI/MTM)_n$. Mechanical properties of the different films were also characterized with nanoindentation. The $(PEI/PAA/PEI/MTM)_n$ system exhibits initial exponential growth followed by linear buildup, but with unusually thick individual bilayers, which were recently reported for a subset of e-LBL

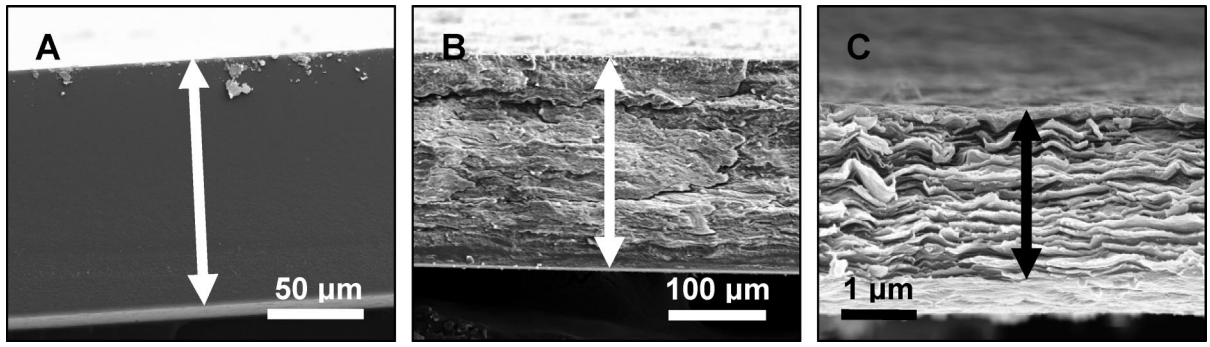

Figure 1. SEM images of cross sections for free-standing films of (A) $(PEI/PAA)_{200}$ with 10 min depositions, (B) $(PEI/PAA/PEI/MTM)_{100}$ with 10 min depositions, and (C) $(PEI/MTM)_{100}$ with 5 min depositions. Arrows indicate span of the cross section.

films incorporating high molecular weight polyelectrolytes.[60] In the present system, the growth rate was established to be nearly identical for $(PEI/PAA/PEI/MTM)_n$ with and without MTM, with total film thicknesses reaching 200 μm for $n =$ 100 and deposition intervals of 10 min, suggesting that inclusion of the MTM nanosheets have surprisingly little effect on the "in-and-out" diffusion mechanism of e-LBL film formation. Similar to the previous publications,[49] fluorescently labeled PEI was found to be diffusing through the film, thus further confirming the "in-and-out" diffusion mechanism. The nanoindentation experiments also showed that the films have unusually high modulus and hardness, which is technologically very important for a variety of coatings. Surprisingly, the properties of the e-LBL films are even higher when compared with the traditional linear systems with much greater inorganic contents and other LBL layers characterized in a similar way before.[82]

In our previous work with $(PDDA/MTM)_n$ thin films, we have shown that the MTM nanosheets interact strongly with the PDDA through a manifold of ionic bonds leading to the formation of nanocomposite with excellent mechanical properties.[69] We have also observed that the MTM nanosheets form a densely packed layer of plates during each adsorption, creating a surface which can be compared to a "ceramic-tile floor". In this structure, the MTM sheets are oriented parallel to the substrate, and in respect to the e-LBL, they are perpendicular to the path of the diffusing polymer. One can wonder what would be the implications for e-LBL process in this system. Most certainly, such orientation appears to hinder the diffusion of macromolecules through the multilayers, which is not favorable to e-LBL. Note that LBL assembly of PEI and PAA has been shown to give exponential growth.[21,67] To answer the questions of feasibility of e-LBL assembly in this system, we have proceeded with the preparation of hybrid films from PEI, as well as purely polymeric films without the MTM inclusions, all in parallel. For comparison, $(PEI/MTM)_n$ films were also prepared.

The films were assembled following similar conditions to the previously reported and well-characterized composite of $(PDDA/MTM)_n$, that is, concentrations of solutions and deposition procedure.[69] Note that pH of the PEI and PAA solutions (see Supporting Information) was adjusted to minimize the charge on the NH_2 and $-COOH$ functional groups in order to decrease the charges on the polymers, which appears to be one of the requirements for the e-LBL process. In a typical assembly, we used 5 min immersion of a glass slide in PEI, 2 min rinse with DI water, 5 min immersion into a PAA, 2 min rinse with DI water, 5 min immersion into a PEI, another 2 min rinse with DI water, a 5 min immersion into a MTM dispersion, followed by a final 2 min rinse with DI water. This sequence after being repeated n times produced $(PEI/PAA/PEI/MTM)_n$ composite. The purely polymeric systems were prepared following the same sequence except that every MTM layer was replaced with a PAA layer, and the same total number of layers was assembled for comparison. One should also keep in mind that the clay-containing e-LBL structures are identical to the $(PDDA/MTM)_n$ or $(PEI/MTM)_n$ except that every other layer of negatively charged MTM has been replaced by negatively charged PAA. To keep the system as close as possible to the previously reported $(PDDA/MTM)_n$, the concentrations and pH's of the polyelectrolytes and MTM solutions were also chosen to be similar to the conditions used in the $(PDDA/MTM)_n$ composites: 0.5 or 1 wt % concentrations (see Supporting Information). For the $(PEI/MTM)_n$ system, we chose 0.1 wt % concentration for PEI since the 1 wt % concentration has led to aggregation at these assembly conditions.

For e-LBL systems with and without clay, a set of 10 films on microscope glass slides with varied number of bilayers, $n = 20-200$, incremented by 20 bilayers was prepared. For $(PEI/MTM)_n$, the films with $n = 100$ and 200 were made. While all of the previous reports dealing with e-LBL have shown films composed of at most 30 bilayers and film thicknesses of no more than 15 μm, we also wanted to see if the exponential growth could be continued to much greater thicknesses. During deposition, within the first few layers, the films became strongly hydrated and had gel-like appearance which was indicative of a successful e-LBL process in accordance with the work by Elbert et al.[45] All of the e-LBL films showed very large thicknesses when hydrated, several millimeters, when compared with the $(PEI/MTM)_n$ or $(PDDA/MTM)_n$. Even upon drying, the thickness of the e-LBL coatings for 200-bilayer films could be easily distinguished with the naked eye (Figure S1, Supportng Information), which otherwise was difficult to observe for the l-LBL, $(PEI/MTM)_n$ films.

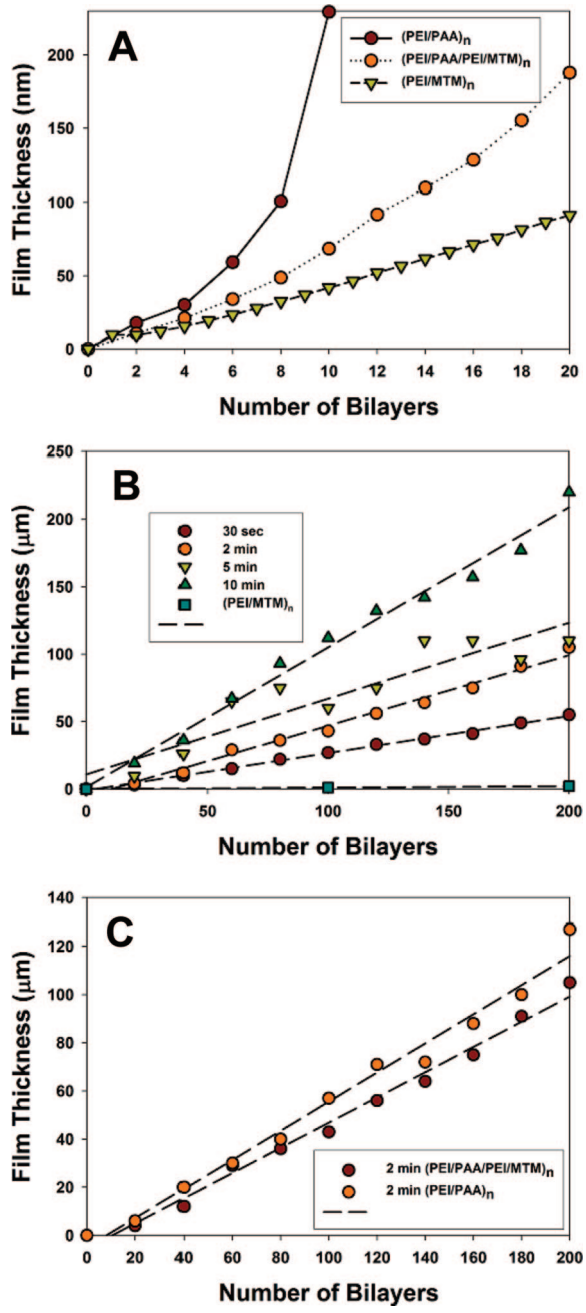

Figure 2. Compilation of thicknesses evolution of e-LBL and l-LBL films as a function of number of deposited layers and with different deposition intervals: (A) Comparison of l-LBL and e-LBL film-growth with and without MTM grown on a silicon wafer with thickness measured using ellipsometry. The "exponential" upswing of the growth curve for $(PEI/PAA/PEI/MTM)_n$ can be clearly seen. The deposition interval for e-LBL films was 2 min, and for the $(PEI/MTM)_n$ it was 5 min. (B) Comparison of thicknesses from SEM for $(PEI/PAA/PEI/MTM)_n$ films with the specified deposition intervals prepared on microscope glass slides. The $(PEI/MTM)_n$ regression is based on the thickness of a 100- and a 200-bilayer film deposited on top of a glass slide with 5 min depositions. (C) Comparison of $(PEI/PAA/PEI/MTM)_n$ with and without MTM following 2 min depositions.

Upon drying, when compared with $(PEI/MTM)_n$, the $(PEI/PAA/PEI/MTM)_n$ films showed extensive cracking (Figure S1). One can speculate that the stresses building up when water is removed from the film constitute the origin of this cracking. The $(PEI/PAA)_n$ films also appeared to be more transparent when compared with the films with MTM. Thermo-gravimetric analysis (TGA) showed the clay content in the dry films to be ~5 wt % at 650 °C (Figure S2), which when normalized for the loss of pure clay at this temperature, it can be estimated as high as ~10 wt %. Overall, similarity of appearance is indicative of the similarity of growth process which can be established more diligently by microscopy and spectroscopy methods.

SEM characterization of the films' cross sections (Figure 1) showed very large thicknesses. For 200-bilayers samples, the measured thicknesses were in excess of 100 μm for the 2, 5, and 10 min depositions. For comparison, $(PDDA/MTM)_n$ films were previously shown to have thicknesses on the order of only ~5 μm for 200 bilayers[69] and the $(PEI/MTM)_n$ showed only ~2 μm for the same number of bilayers. From the structural point of view, $(PEI/PAA)_n$ films (Figure 1A) had very uniform and homogeneous image of the cross section. The films with MTM (Figure 1B and Figure S3) showed architecture with indications of stratification. This architecture is also very different when compared with the well-defined and layered structure of $(PEI/MTM)_n$ films (Figure 1C). Overall, on the basis of these SEM data, one must conclude that, indeed, the MTM platelets were successfully incorporated into the e-LBL structure.

In addition to the large thicknesses, further proof of the exponential process was obtained from ellipsometric measurements of film growth on top of polished silicon surfaces (Figure 2A). For the e-LBL films, both of the curves show a clear upswing, especially when compared with the l-LBL, $(PEI/MTM)_n$. Notably, the total film thickness for the film studied with ellipsometry is more than 10 times smaller as that of the film grown for SEM/optical studies. While an exponential trend is unmistakable, it is less pronounced than for the $(PEI/PAA)_n$. Here, it would be appropriate to notice that drying is a critical parameter in the e-LBL and for MTM-containing layers in particular. While the films used for ellipsometry were dried after every deposition cycle, that is, $(PEI/PAA/PEI/MTM)_1$ sequence, the films grown on top of the glass slides were only dried at the end of the process. For comparison, a film prepared with drying after every single deposited material layer showed completely linear growth for the same number of layers.

After the initial exponential regime, the growth appears to be relatively constant and linear. This is especially evident from the plots of thicknesses of the prepared film sets as a function of number of bilayers in Figure 2B. All of the films show linear growth however with very large increments. The same behavior was recently demonstrated for e-LBL films composed of high molecular weight polyelectrolytes.[60] Porcel et al. have shown that the e-LBL system will transition to a thick l-LBL with increasing molecular weight of the polymers. Note that the slope of this linear portion of e-LBL is strongly dependent on the length of the deposition interval. Varying the deposition from 30 s to 10 min gave substantial changes in the total thicknesses of the films (Figure 2B) as well as the thicknesses of the individual polyelectrolyte complex layers. This observation suggested that the saturation

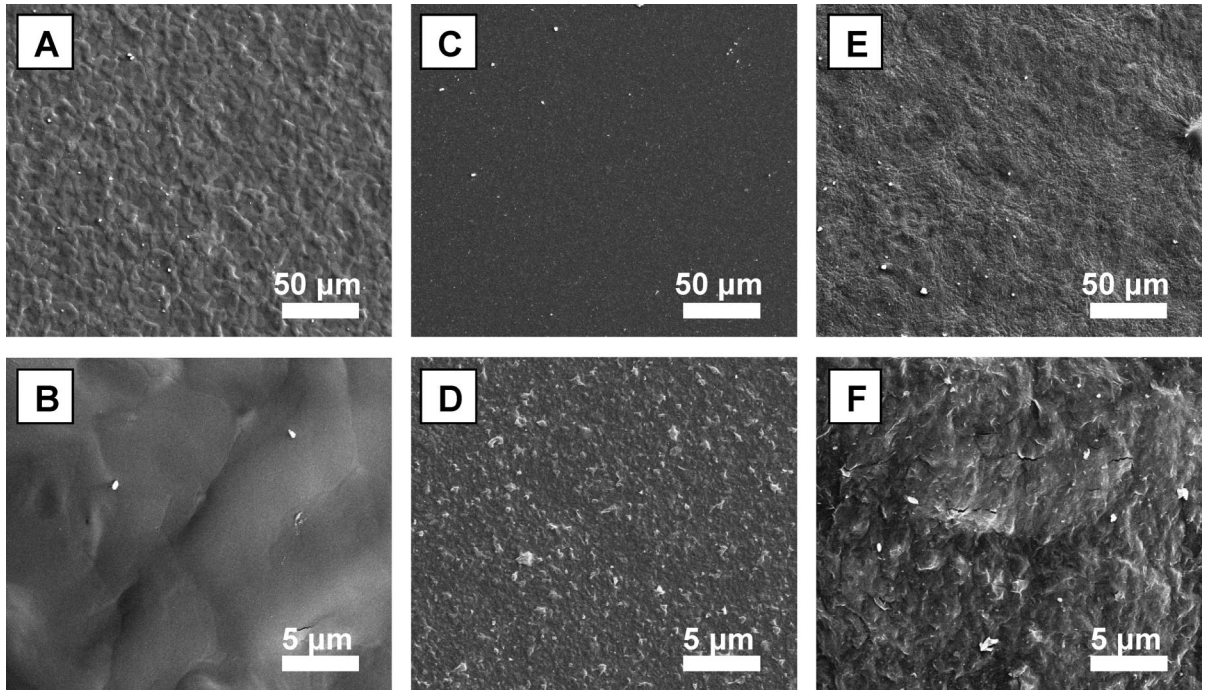

Figure 3. SEM comparison of top surface morphologies for (A,B) $(PEI/PAA)_{20}$, (C,D) $(PEI/MTM)_{20}$, and (E,F) $(PEI/PAA/PEI/MTM)_{10}$ films.

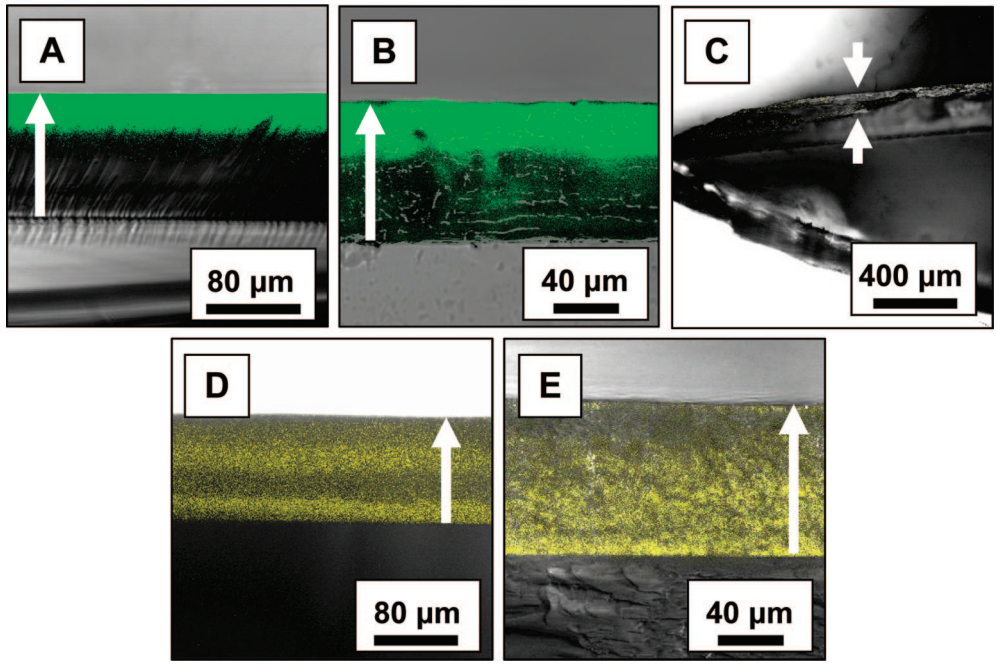

Figure 4. Laser scanning confocal microscopy characterization of dye-labeled polymer diffusion in the e-LBL systems. (A,B) $(PEI/PAA)_{200}$ and $(PEI/PAA/PEI/MTM)_{100}$with top layer of FITC-PEI, respectively. (C) $(PEI/PAA/PEI/MTM)_{100}$ control without labeled polymers. (D,E) $(PEI/PAA/PEI/MTM)_{100}$, and $(PEI/PAA)_{200}$ with top layer of LYC-PAA, respectively. White arrow indicates growth direction of the film.

of the film has not been reached in the allotted amount of time. The dependence on the lifetime is also indicative of the diffusion-limited nature of growth pattern.

While transition from e-LBL to l-LBL with large thicknesses of layers added in each deposition cycle is not surprising, the question arises whether MTM slows down this stage of LBL growth due to retarded diffusion of a polyelectrolyte through the MTM layers. However side-by-side comparison of films with and without MTM (Figure 2C) showed nearly identical growth kinetics. The cumulative conclusion that one can reach is that, apart from greater sensitivity to drying (Figure 2A), the growth process in $(PEI/PAA)_n$ and $(PEI/PAA/PEI/MTM)_n$ systems is quite similar regardless of incorporation of a significant amount of alumosilicate in the fabric of the film.

Comparison of the top surface morphologies by SEM for the dried films of $(PEI/PAA)_{20}$, $(PEI/MTM)_{20}$, and $(PEI/PAA/PEI/MTM)_{10}$ (Figure 3) shows striking differences between

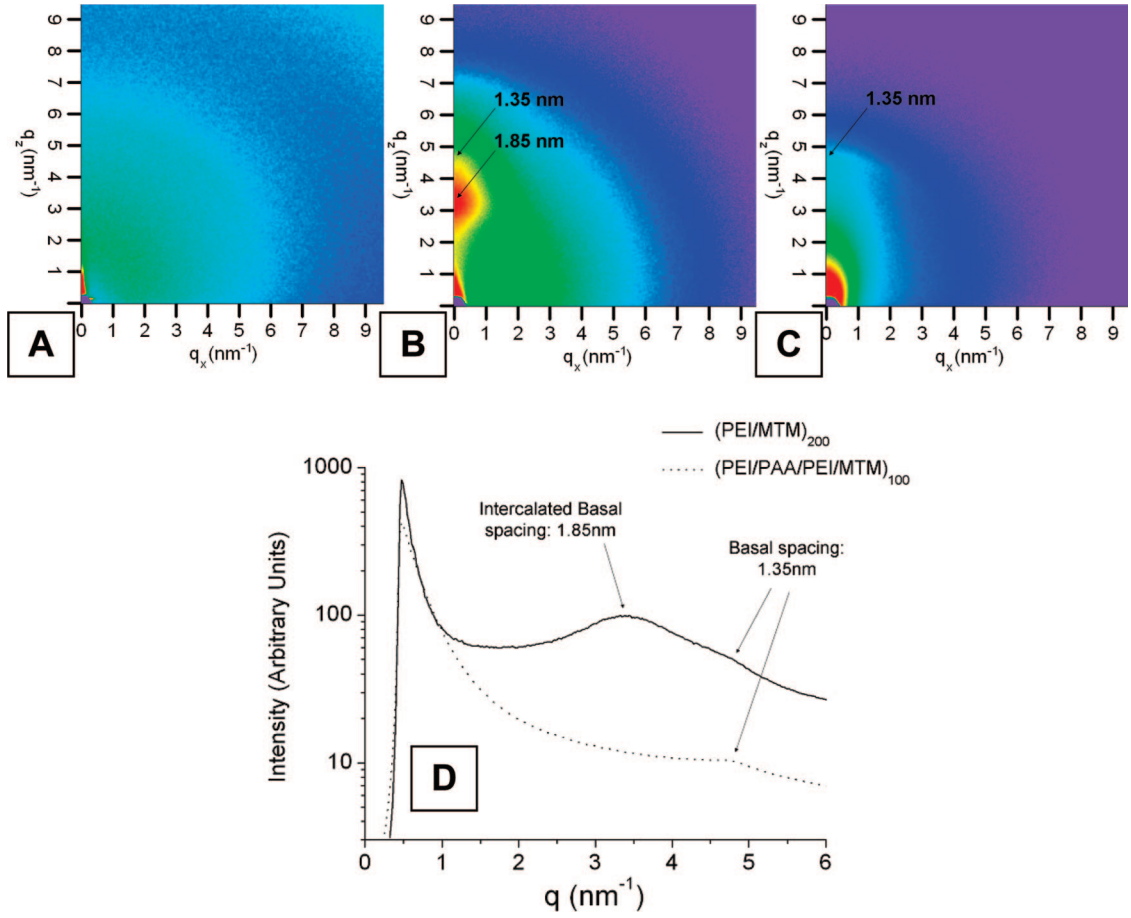

Figure 5. 2-D SAXS patterns of free-standing films of (A) $(PEI/PAA)_{200}$, (B) $(PEI/MTM)_{200}$, and (C) $(PEI/PAA/PEI/MTM)_{100}$. The scattering features of interest are indicated by arrows and the corresponding spacings are noted. (D) 1-D SAXS patterns of free-standing films of $(PEI/MTM)_{200}$ and $(PEI/PAA/PEI/MTM)_{100}$. These plots are radial integrations of the 2-D images shown in B and C. The intensities were shifted for clarity. The intercalated basal spacing of 1.85 nm is clearly observed in the PEI/MTM film, and weak basal spacings of 1.35 nm are observed in both films. The lack of intense scattering from the montmorillonite in the PEI/PAA/PEI/MTM film indicates either a wide range of intercalated basal spacings or exfoliation of the clay platelets.

the three systems and gives some explanation for the distorted internal architecture in the $(PEI/PAA/PEI/MTM)_n$ system (Figure 1B). At low magnification, the $(PEI/MTM)_{20}$ film shows relatively flat surface topography (Figure 3C) when compared with its e-LBL counterparts, which is indicative of uniform distribution and parallel orientation of the platelets on the substrate. At higher magnification (Figure 3D), the presence of MTM platelets is revealed, also showing some adsorbed aggregates. The e-LBL films with and without MTM inclusions show strong, yet uniform roughness even at low magnification which presumably is a result of rapid shrinking and non-uniform stresses in the film when drying the highly swollen structure. In the films containing MTM, during shrinking, the adsorbed platelets, because of their significantly smaller size, orient themselves parallel to the roughened surface, thus acquiring three-dimensional (3-D) conformation. This "pseudo"-3-D orientation of MTM (unlike largely parallel-to-substrate orientation of platelets seen typically in LBL films of clays) further can be the cause and/or be a result of the diffusion of polylectrolytes.

On the basis of the previous studies by Picart et al.,[49] one can expect that the mechanism of the exponential growth in $(PEI/PAA/PEI/MTM)_n$ films can be described as the following. PEI, being a polycation, diffuses into the matrix of the previously deposited layer in the amount substantially above the limits of electroneutrality. Swelling of the films can be the cause of as well as the reason for the accumulation of PEI in the composite. To some degree, the fast diffusion of the polyelectrolytes can be explained by reptation movements of similar polymers previously observed for LBL films with nanoparticles.[83] When the film is exposed to PAA or MTM, the stored amount of PEI diffuses out and forms a polyelectrolyte complex on the surface of the multilayers with PAA or MTM.

Verification of the diffusion mechanism suggested was attained in a similar fashion to previous works[46] but not without unexpected findings. PEI and PAA polymers have been conjugated with fluorescein isothiocyanate isomer I (FITC) and *N*-(5-aminopentyl)-4-amino-3,6- disulfo-1,8-naphthalimide, dipotassium salt (lucifer yellow cadaverine, LYC) fluorescent dyes, respectively (see Supporting Information), and their diffusion through the films was observed with confocal microscopy. In this experiment, we have immersed a glass slide coated with a 200-bilayer e-LBL film of each structure into a dye-labeled polyelectrolyte for 30 min, and after rinsing and drying, we have imaged the cross

section of the film. Similarly to all previous publications on e-LBL, all of the films showed diffusion of the polycation (Figure 4A and B), which certainly confirms the e-LBL mechanism for MTM-containing multilayers. Note that even for the 30 min, the diffusion extends only through a portion of the film and between the two systems; the depth of diffusion is nearly identical at ~30 and 27 μm. This is consistent with the molecular weight dependence of the diffusion as in Figure 2A and inability of the multilayer matrix to reach saturation of PEI accumulation, which leads to the seemingly linearly growing e-LBL producing very thick films.[60]

Interestingly, PAA seemed to have diffused throughout the film (Figure 4D, E) as well. Although there is no obvious fundamental restriction that polyanions cannot diffuse through the matrix of LBL layers, such process was previously underestimated for e-LBL layers although indications that it does take place were reported.[29,84] To some degree, this changes significantly the mechanism that can be suggested on the basis of literature data exclusively and the need to foresee the possibility of PAA incorporation and diffusion out similarly to what was described for PEI above.

To answer the question of how the PEI and PAA is able to diffuse through the tightly packed clay layers, one needs to better understand the organization of clay sheets in order to resolve the question about permeability of the polyelectrolytes through them. It can be done by using small-angle X-ray scattering (SAXS) revealing the information about internal layering morphologies of $(PEI/PAA)_n$, $(PEI/MTM)_n$, and $(PEI/PAA/PEI/MTM)_n$ films (Figure 5). The $(PEI/PAA)_n$ film does not contain clay, and thus only diffuse scattering from the polymers is observed (Figure 5A). For the films containing clay, the primary peak observed in the $(PEI/MTM)_n$ film corresponds to a basal spacing of 1.85 nm (Figure 5B,D), indicating significant intercalation of polymer between clay sheets. A smaller shoulder was observed indicating the presence of a smaller basal spacing at 1.35 nm, which is similar to literature values of the basal spacing for Na^+-montmorillonite.[85] Importantly, the $(PEI/PAA/PEI/MTM)_n$ film only displays a weak peak corresponding to a basal spacing of 1.35 nm indicative of a lower degree of organization (Figure 5C,D).

The intensity of SAXS peak in the $(PEI/MTM)_n$ film is much stronger (Figure 5D), indicating a more regular structure. The lack of intense scattering from the montmorillonite in the $(PEI/PAA/PEI/MTM)_n$ film indicates either a wide range of intercalated basal spacings or exfoliation of the clay platelets. In the $(PEI/MTM)_n$ film, the positively charged PEI intercalates the montmorillonite interlayer gallery by exchanging with the Na^+ ions. In this case, any further intercalation of PEI into the interlayer gallery will lead to an excess positive charge. Considering diffusion data in Figure 4 and SAXS results, one can also suggest the possibility of PAA diffusing into the interlayer gallery of $(PEI/PAA/PEI/MTM)_n$, especially when a large amount of PEI is accumulated in the matrix, allowing further separation of the alumosilicate sheets and corresponding larger spread of basal spacing values.

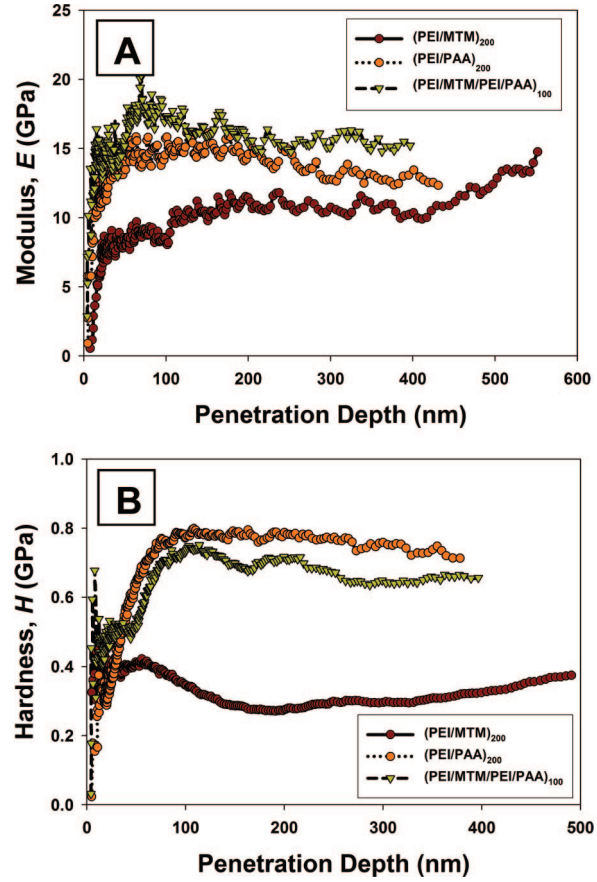

Figure 6. Typical results from nanoindentation experiments for $(PEI/MTM)_{200}$, $(PEI/PAA)_{200}$, and $(PEI/MTM/PEI/PAA)_{100}$ films with 5 min, 2 min, and 10 min depositions, respectively. (A) Represents the modulus as a function of penetration depth (B) Corresponding hardness. These results are from the "loading" (penetration as opposed to retraction of the tip) part of the experiment and the maximum load-to force was set at 2 mN, hence the different number of experimental points.

We can further quantify the orientation of the clay platelets by using Herman's orientation parameter (f).[86–88] To calculate the orientation parameter, azimuthal scans were taken over a small window around the q value. This parameter ranges from 1 to $-1/2$, in which a value of zero indicates a completely random distribution of orientations. When f is 1 or $-1/2$, the system is completely aligned parallel or perpendicular, respectively, to the chosen reference direction (in this case, normal to the substrate). The values for the orientation parameter were as follows: $(PEI/MTM)_n$ for spacing between 1.3 and 1.4 nm, 0.27 ± 0.07; $(PEI/MTM)_n$ for spacings between 1.8 and 1.9 nm, 0.46 ± 0.07; and $(PEI/PAA/PEI/MTM)_n$ with MTM for spacing between 1.3 and 1.4 nm, 0.27 ± 0.10.

These trends agree well with visual inspection of the SEM images in Figures 1 and 2: the MTM platelets in the $(PEI/MTM)_n$ sample are clearly more oriented parallel to the substrate than in the $(PEI/PAA/PEI/MTM)_n$ sample, thus corroborating the SAXS data.

Last, in addition to the dynamics of growth and the structure in these hybrid e-LBL films, we have investigated their mechanical properties as they are of great interest for accelerating the preparation process of the ultrastrong nano-

Table 1. Experimental Results from Comparison of the Mechanical Properties of (PDDA/MTM), (PEI/MTM), (PEI/PAA), and (PEI/MTM/PEI/PAA) LBL Films Using Nanoindentation[a]

	Loading		Unloading	
sample type	modulus, E (GPa)	hardness, H (GPa)	modulus, E (GPa)	hardness, H (GPa)
PDDA/MTM	9.5	0.46		
PEI/MTM	13.7 ± 0.5	0.49 ± 0.22	16.9 ± 0.2	0.50 ± 0.22
PEI/PAA	15.4 ± 3.0	0.70 ± 0.23	17.0 ± 0.2	0.67 ± 0.21
PEI/MTM/PEI/MTM	15.7 ± 5.1	0.88 ± 0.45	21.4 ± 0.8	0.98 ± 0.81

[a] Data for (PDDA/MTM) are taken from Fan et al.[82]

composites. Since this family of e-LBL films displayed extensive cracking (other combinations were found to be very stable in dry conditions), we found the nanoindentation technique to be the most suitable to perform these measurements (see Supporting Information). The nanoindentation also allowed us to make a comparison with previous such studies on PDDA/MTM films. Previously, Advincula et al. demonstrated that the PDDA/MTM films possess modulus of $E = 9.5$ GPa, and hardness of $H = 0.46$ GPa.[82] In that study, the authors found that the hardness of $(PDDA/MTM)_{100}$ films was higher than the hardness of some of the high strength polymers, for example, isotactic polypropylene ($H = 0.125$ GPa) and high density polyethylene ($H = 0.06$ GPa), and it was on par with a soft metal, copper, ($H = 0.46$ GPa).[82,89] To our surprise, the e-LBL films also showed exceptionally high modulus and hardness, in spite of having much lower content of the very stiff MTM platelets (Figure 6).

In this experiment we have compared films of $(PEI/MTM)_{200}$, $(PEI/PAA)_{200}$, and $(PEI/MTM/PEI/PAA)_{100}$ with 5 min, 2 min, and 10 min depositions. For each of the samples, experimental data for an array of 3×3 indents were collected and results from loading and unloading parts of the force-displacement curves were compared. The experimental results are summarized in Table 1, and they are compared to the previous results for $(PDDA/MTM)_n$ film.

The experimental data show that the $(PEI/MTM)_n$ and $(PDDA/MTM)_n$ films have relatively similar properties. Surprisingly, the e-LBL films with and without MTM inclusions have actually higher stiffness and hardness than those growing in nonexponential mechanism. This is a most unpredictable result since the loading of clay nanosheets in the e-LBL film is an order of magnitude lower than in the l-LBL structures. The explanation for this phenomenon is likely to be the fact that dynamic nature of e-LBL films allows the polymer to adjust to nanoscale topography of the clay sheets and/or the partner polymer better than in l-LBL. Such "molecular fitting" of the more flexible component to the other was shown to be critical for obtaining high mechanical properties.[71,72]

In conclusion, the results presented here are the first example of exponentially growing LBL structures incorporating inorganic sheet-like nanoparticles. These findings open up the door to a much greater research avenue into hybrid organic/inorganic exponential LBL structures. It was demonstrated that clay sheets despite their well-known barrier function, do not prevent exponential growth of LBL films. The explanation for exponential growth phenomenon can come from the unexpectedly fast diffusion/reptation through the openings between the MTM tiles. This process is aided by a slight tilt of clay sheets when PAA is present in the system. Along with faster growth multilayers, the e-LBL mechanism also gives substantial as well as unpredictable improvement in mechanical properties, which was attributed to the closer approach to thermodynamic equilibrium in a system with greater molecular mobility. The mechanism(s) described here also have a great importance for acceleration of the manufacturing of layered composites with unique mechanical properties.

Acknowledgment. N.A.K. thanks AFOSR, NSF, DARPA, and NRL for the support of this research. P.P. thanks the Fannie and John Hertz Foundation for support of his work through a graduate fellowship. Authors acknowledge the staff of the Electron Microscopy Analysis Laboratory (University of Michigan) and their sponsor, National Science Foundation (NSF) through Grant #DMR-0320740. M.M. acknowledges the Fulbright fellowship. N.W.S.K. acknowledges the Michigan Society of Fellows. V.B. acknowledges the "Commission Franco-Américaine", the Fulbright Foundation, and Région Alsace for financial support. E.V. and A.J.H. thank the Cornell High Energy Synchrotron Source (CHESS), which is supported by the National Science Foundation and the National Institutes of Health/National Institute of General Medical Sciences under Award No. DMR-0225180. E.V. thanks funding from MIT's Institute for Soldier Nanotechnology (ISN).

Supporting Information Available: Experimental details, optical images of exponentially grown films, TGA analysis results, SEM images. This material is available free of charge via the Internet at http://pubs.acs.org.

References

(1) Iler, R. K.; Colloid, J. *Interface Sci.* **1966**, *21*, 569.
(2) Decher, G.; Schmitt, J. *Prog. Coll. Pol. Sci.* **1992**, *89*, 160.
(3) Decher, G. *Science* **1997**, *277*, 1232.
(4) Hammond, P. T. *Adv. Mater.* **2004**, *16*, 1271.
(5) Ingersoll, D.; Kulesza, P. J.; Faulkner, L. R. *J. Electrochem. Soc.* **1994**, *141*, 140.
(6) Kotov, N. A.; Dekany, I.; Fendler, J. H. *J. Phys. Chem.* **1995**, *99*, 13065.
(7) Mamedov, A. A.; Kotov, N. A.; Prato, M.; Guldi, D. M.; Wicksted, J. P.; Hirsch, A. *Nat. Mater.* **2002**, *1*, 190.
(8) Jiang, C.; Ko, H.; Tsukruk, V. V. *Adv. Mater.* **2005**, *17*, 2127.
(9) Keller, S. W.; Kim, H. N.; Mallouk, T. E. *J. Am. Chem. Soc.* **1994**, *116*, 8817.
(10) Cooper, T. M.; Campbell, A. L.; Crane, R. L. *Langmuir* **1995**, *11*, 2713.
(11) Podsiadlo, P.; Choi, S. Y.; Shim, B.; Lee, J.; Cuddihy, M.; Kotov, N. A. *Biomacromolecules* **2005**, *6*, 2914.

(12) Podsiadlo, P.; Sui, L.; Elkasabi, Y.; Burgardt, P.; Lee, J.; Miryala, A.; Kusumaatmaja, W.; Carman, M. R.; Shtein, M.; Kieffer, J.; Lahann, J.; Kotov, N. A. *Langmuir* **2007**, *23*, 7901.
(13) He, J. A.; Valluzzi, R.; Yang, K.; Dolukhanyan, T.; Sung, C.; Kumar, J.; Tripathy, S. K.; Samuelson, L.; Balogh, L.; Tomalia, D. A. *Chem. Mater.* **1999**, *11*, 3268.
(14) Araki, K.; Wagner, M. J.; Wrighton, M. S. *Langmuir* **1996**, *12*, 5393.
(15) Lvov, Y.; Onda, M.; Ariga, K.; Kunitake, T. *J. Biomat. Sci.: Polym. E.* **1998**, *9*, 345.
(16) Richert, L.; Lavalle, P.; Vautier, D.; Senger, B.; Stoltz, J. F.; Schaaf, P.; Voegel, J. C.; Picart, C. *Biomacromolecules* **2002**, *3*, 1170.
(17) Boulmedais, F.; Ball, V.; Schwinte, P.; Frisch, B.; Schaaf, P.; Voegel, J. C. *Langmuir* **2003**, *19*, 440.
(18) Lvov, Y.; Decher, G.; Sukhorukov, G. *Macromolecules* **1993**, *26*, 5396.
(19) Hong, J. D.; Lowack, K.; Schmitt, J.; Decher, G. *Prog. Coll. Pol. Sci.* **1993**, *93*, 98.
(20) Lvov, Y.; Ariga, K.; Kunitake, T. *Chem. Lett.* **1994**, (12), 2323.
(21) Yoo, P. J.; Nam, K. T.; Qi, J.; Lee, S. K.; Park, J.; Belcher, A. M.; Hammond, P. T. *Nat. Mater.* **2006**, *5*, 234.
(22) Tang, Z.; Wang, Y.; Podsiadlo, P.; Kotov, N. A. *Adv. Mater.* **2006**, *18*, 3203.
(23) Kotov, N. A. Ordered layered assemblies of nanoparticles. *MRS Bull.* **2001**, *26*, 992.
(24) Zhai, L.; Cebeci, F. C.; Cohen, R. E.; Rubner, M. F. *Nano Lett.* **2004**, *4*, 1349.
(25) Zhai, L.; Berg, M. C.; Cebeci, F. C.; Kim, Y.; Milwid, J. M.; Rubner, M. F.; Cohen, R. E. *Nano Lett.* **2006**, *6*, 1213.
(26) Ellis, D. L.; Zakin, M. R.; Bernstein, L. S.; Rubner, M. F. *Anal. Chem.* **1996**, *68*, 817.
(27) Constantine, C. A.; Mello, S. V.; Dupont, A.; Cao, X.; Santos, D., Jr.; Oliveira, O. N., Jr.; Strixino, F. T.; Pereira, E. C.; Cheng, T.; Defrank, J. J.; Leblanc, R. M. *J. Am. Chem. Soc.* **2003**, *125*, 1805.
(28) Koktysh, D. S.; Liang, X.; Yun, B. G.; Pastoriza-Santos, I.; Matts, R. L.; Giersig, M.; Serra-Rodriguez, C.; Liz-Marzan, L. M.; Kotov, N. A. *Adv. Funct. Mater.* **2002**, *12*, 255.
(29) Wood, K. C.; Chuang, H. F.; Batten, R. D.; Lynn, D. M.; Hammond, P. T. *Proc. Natl. Acad. Sci. U.S.A.* **2006**, *103*, 10207.
(30) Jewell, C. M.; Zhang, J.; Fredin, N. J.; Lynn, D. M. *J. Controlled Release* **2005**, *106*, 214.
(31) Lee, J. S.; Cho, J.; Lee, C.; Kim, I.; Park, J.; Kim, Y. M.; Shin, H.; Lee, J.; Caruso, F. *Nat. Nanotech.* **2007**, *2*, 790.
(32) Hiller, J.; Mendelsohn, J. D.; Rubner, M. F. *Nat. Mater.* **2002**, *1*, 59.
(33) DeLongchamp, D. M.; Hammond, P. T. *Adv. Funct. Mater.* **2004**, *14*, 224.
(34) Moriguchi, I.; Fendler, J. H. *Chem. Mater.* **1998**, *10*, 2205.
(35) Heuberger, R.; Sukhorukov, G.; Voeroes, J.; Textor, M.; Moehwald, H. *Adv. Funct. Mater.* **2005**, *15*, 357.
(36) Tokuhisa, H.; Hammond, P. T. *Adv. Funct. Mater.* **2003**, *13*, 831.
(37) Zhang, J.; Senger, B.; Vautier, D.; Picart, C.; Schaaf, P.; Voegel, J. C.; Lavalle, P. *Biomaterials* **2005**, *26*, 3353.
(38) Mamedov, A. A.; Belov, A.; Giersig, M.; Mamedova, N. N.; Kotov, N. A. *J. Am. Chem. Soc.* **2001**, *123*, 7738.
(39) Wang, D.; Rogach, A. L.; Caruso, F. *Nano Lett.* **2002**, *2*, 857.
(40) Liu, J.; Cheng, L.; Song, Y.; Liu, B.; Dong, S. *Langmuir* **2001**, *17*, 6747.
(41) Shen, Y.; Liu, J.; Jiang, J.; Liu, B.; Dong, S. *J. Phys. Chem. B* **2003**, *107*, 9744.
(42) Nolte, A. J.; Rubner, M. F.; Cohen, R. E. *Langmuir* **2004**, *20*, 3304.
(43) Mamedov, A. A.; Kotov, N. A. *Langmuir* **2000**, *16*, 5530.
(44) Shim, B. S.; Podsiadlo, P.; Lilly, D. G.; Agarwal, A.; Lee, J.; Tang, Z.; Ho, S.; Ingle, P.; Paterson, D.; Lu, W.; Kotov, N. A. *Nano Lett.* **2007**, *7*, 3266.
(45) Elbert, D. L.; Herbert, C. B.; Hubbell, J. A. *Langmuir* **1999**, *15*, 5355.
(46) Ruths, J.; Essler, F.; Decher, G.; Riegler, H. *Langmuir* **2000**, *16*, 8871.
(47) Pardo-Yissar, V.; Katz, E.; Lioubashevski, O.; Willner, I. *Langmuir* **2001**, *17*, 1110.
(48) Picart, C.; Lavalle, P.; Hubert, P.; Cuisinier, F. J. G.; Decher, G.; Schaaf, P.; Voegel, J. C. *Langmuir* **2001**, *17*, 7414.
(49) Picart, C.; Mutterer, J.; Richert, L.; Luo, Y.; Prestwich, G. D.; Schaaf, P.; Voegel, J. C.; Lavalle, P. *Proc. Natl. Acad. Sci. U.S.A.* **2002**, *99*, 12531.
(50) Lavalle, P.; Gergely, C.; Cuisinier, F. J. G.; Decher, G.; Schaaf, P.; Voegel, J. C.; Picart, C. *Macromolecules* **2002**, *35*, 4458.
(51) Lavalle, P.; Picart, C.; Mutterer, J.; Gergely, C.; Reiss, H.; Voegel, J. C.; Senger, B.; Schaaf, P. *J. Phys. Chem. B* **2004**, *108*, 635.
(52) Lavalle, P.; Vivet, V.; Jessel, N.; Decher, G.; Voegel, J. C.; Mesini, P. J.; Schaaf, P. *Macromolecules* **2004**, *37*, 1159.
(53) Garza, J. M.; Schaaf, P.; Muller, S.; Ball, V.; Stoltz, J. F.; Voegel, J. C.; Lavalle, P. *Langmuir* **2004**, *20*, 7298.
(54) Garza, J. M.; Jessel, N.; Ladam, G.; Dupray, V.; Muller, S.; Stoltz, J. F.; Schaaf, P.; Voegel, J. C.; Lavalle, P. *Langmuir* **2005**, *21*, 12372.
(55) Huebsch, E.; Ball, V.; Senger, B.; Decher, G.; Voegel, J. C.; Schaaf, P. *Langmuir* **2004**, *20*, 1980.
(56) Porcel, C.; Lavalle, P.; Ball, V.; Decher, G.; Senger, B.; Voegel, J. C.; Schaaf, P. *Langmuir* **2006**, *22*, 4376.
(57) Ball, V.; Huebsch, E.; Schweiss, R.; Voegel, J. C.; Schaaf, P.; Knoll, W. *Langmuir* **2005**, *21*, 8526.
(58) Huebsch, E.; Fleith, G.; Fatisson, J.; Labbe, P.; Voegel, J. C.; Schaaf, P.; Ball, V. *Langmuir* **2005**, *21*, 3664.
(59) Kujawa, P.; Moraille, P.; Sanchez, J.; Badia, A.; Winnik, F. M. *J. Am. Chem. Soc.* **2005**, *127*, 9224.
(60) Porcel, C.; Lavalle, P.; Decher, G.; Senger, B.; Voegel, J. C.; Schaaf, P. *Langmuir* **2007**, *23*, 1898.
(61) Nam, K. T.; Kim, D. W.; Yoo, P. J.; Chiang, C. Y.; Meethong, N.; Hammond, P. T.; Chiang, Y. M.; Belcher, A. M. *Science* **2006**, *312*, 885.
(62) Eriksson, M.; Notley, S. M.; Wagberg, L. *J. Colloid Interface Sci.* **2005**, *292*, 38.
(63) Vodouhe, C.; Le Guen, E.; Garza, J. M.; Francius, G.; Dejugnat, C.; Ogier, J.; Schaaf, P.; Voegel, J. C.; Lavalle, P. *Biomaterials* **2006**, *27*, 4149.
(64) Jessel, N.; Oulad-Abdelghani, M.; Meyer, F.; Lavalle, P.; Haikel, Y.; Schaaf, P.; Voegel, J. C. *Proc. Natl. Acad. Sci. U.S.A.* **2006**, *103*, 8618.
(65) Boulmedais, F.; Tang, C. S.; Keller, B.; Voros, J. *Adv. Funct. Mater.* **2006**, *16*, 63.
(66) Dimitrova, M.; Arntz, Y.; Lavalle, P.; Meyer, F.; Wolf, M.; Schuster, C.; Haikel, Y.; Voegel, J. C.; Ogier, J. *Adv. Funct. Mater.* **2007**, *17*, 233.
(67) Ji, J.; Fu, J.; Shen, J. *Adv. Mater.* **2006**, *18*, 1441.
(68) Mertz, D.; Hemmerle, J.; Mutterer, J.; Ollivier, S.; Voegel, J. C.; Schaaf, P.; Lavalle, P. *Nano Lett.* **2007**, *7*, 657.
(69) Tang, Z.; Kotov, N. A.; Magonov, S.; Ozturk, B. *Nat. Mater.* **2003**, *2*, 413.
(70) Podsiadlo, P.; Liu, Z.; Paterson, D.; Messersmith, P. B.; Kotov, N. A. *Adv. Mater.* **2007**, *19*, 949.
(71) Podsiadlo, P.; Tang, Z.; Shim, B. S.; Kotov, N. A. *Nano Lett.* **2007**, *7*, 1224.
(72) Podsiadlo, P.; Kaushik, A. K.; Arruda, E. M.; Waas, A. M.; Shim, B. S.; Xu, J.; Nandivada, H.; Pumplin, B. G.; Lahann, J.; Ramamoorthy, A.; Kotov, N. A. *Science* **2007**, *318*, 80.
(73) Podsiadlo, P.; Paternel, S.; Rouillard, J. M.; Zhang, Z.; Lee, J.; Lee, J. W.; Gulari, E.; Kotov, N. A. *Langmuir* **2005**, *21*, 11915.
(74) Malikova, N.; Pastoriza-Santos, I.; Schierhorn, M.; Kotov, N. A.; Liz-Marzan, L. M. *Langmuir* **2002**, *18*, 3694.
(75) Lvov, Y.; Ariga, K.; Ichinose, I.; Kunitake, T. *J. Am. Chem. Soc.* **1995**, *117*, 6117.
(76) Ku, B. C.; Froio, D.; Steeves, D.; Kim, D. W.; Ahn, H.; Ratto, J. A.; Blumstein, A.; Kumar, J.; Samuelson, L. A. *J. Macromol. Sci. A* **2004**, *A41*, 1401.
(77) Kim, D. W.; Choi, H. S.; Lee, C.; Blumstein, A.; Kang, Y. *Electrochim. Acta* **2004**, *50*, 659.
(78) Guo, Z.; Shen, Y.; Zhao, F.; Wang, M.; Dong, S. *Analyst* **2004**, *129*, 657.
(79) Yamamoto, T.; Umemura, Y.; Sato, O.; Einaga, Y. *Chem. Lett.* **2004**, *33*, 500.
(80) Li, Z.; Hu, N. *J. Electroanal. Chem.* **2003**, *558*, 155.
(81) Kotov, N. A.; Magonov, S.; Tropsha, E. *Chem. Mater.* **1998**, *10*, 886.
(82) Fan, X.; Park, M. K.; Xia, C.; Advincula, R. *J. Mater. Res.* **2002**, *17*, 1622.
(83) Tang, Z.; Wang, Y.; Kotov, N. A. *Langmuir* **2002**, *18*, 7035.
(84) Sun, B.; Jewell, C. M.; Fredin, N. J.; Lynn, D. M. *Langmuir* **2007**, *23*, 8452.
(85) Brown, G. *The X-ray Identification and Crystal Structures of Clay Minerals*; Mineralogical Society: London, 1961.
(86) Roe, R.-J. *Methods of X-ray and Neutron Scattering in Polymer Science*; Oxford University Press: New York, 2000.
(87) Finnigan, B.; Jack, K.; Campbell, K.; Halley, P.; Truss, R.; Casey, P.; Cookson, D.; King, S.; Martin, D. *Macromolecules* **2005**, *38*, 7386.
(88) Lutkenhaus, J. L.; Olivetti, E. A.; Verploegen, E. A.; Cord, B. M.; Sadoway, D. R.; Hammond, P. T. *Langmuir* **2007**, *23*, 8515.
(89) Gracias, D. H.; Somorjai, G. A. *Macromolecules* **1998**, *31*, 1269.

NL8011648